# Mechanism of lipid-body formation in prokaryotes: how bacteria fatten up

Marc Wältermann,<sup>1</sup> Andreas Hinz,<sup>2</sup> Horst Robenek,<sup>3</sup> David Troyer,<sup>3</sup> Rudolf Reichelt,<sup>4</sup> Ursula Malkus,<sup>4</sup> Hans-Joachim Galla,<sup>2</sup> Rainer Kalscheuer,<sup>1</sup> Tim Stöveken,<sup>1</sup> Philipp von Landenberg<sup>5</sup> and Alexander Steinbüchel<sup>1\*</sup>

<sup>1</sup>Institut für Molekulare Mikrobiologie und Biotechnologie, <sup>2</sup>Institut für Biochemie, <sup>3</sup>Institut für Arterioskleroseforschung, Abteilung für Zellbiologie und Ultrastrukturforschung, <sup>4</sup>Institut für Medizinische Physik und Biophysik, Elektronenmikroskopie und Analytik, Universitätsklinikum Münster, Westfälische Wilhelms-Universität, D-48149 Münster, Germany. <sup>5</sup>Institut für Klinische Chemie und Laboratoriumsmedizin, Johannes Gutenberg Universität Mainz, D-55101 Mainz, Germany.

#### Summary

Neutral lipid accumulation is frequently observed in some Gram-negative prokaryotes like Acinetobacter sp. and most actinomycetes, including the pathogenic Mycobacterium tuberculosis and antibiotic producing streptomycetes. We examined the formation of wax ester- and triacylglycerol (TAG)-bodies in Acinetobacter calcoaceticus and Rhodococcus opacus using microscopic, immunological and biophysical methods. A general model for prokaryotic lipid-body formation is proposed, clearly differing from the current models for the formation of lipid inclusions in eukaryotes and of poly(hydroxyalkanoic acid) (PHA) inclusions in prokaryotes. Formation of lipid-bodies starts with the docking of wax ester synthase/acyl-CoA:diacylglycerol acyltransferase (WS/DGAT) to the cytoplasm membrane. Both, analyses of in vivo and in vitro lipid-body synthesis, demonstrated the formation of small lipid droplets (SLDs), which remain bound to the membraneassociated enzyme. SLDs conglomerated subsequently to membrane-bound lipid-prebodies which are then released into the cytoplasm. The formation of matured lipid-bodies in the cytoplasm occurred by means of coalescence of SLDs inside the lipid

Accepted 18 October, 2004. \*For correspondence. E-mail steinbu@uni-muenster.de; Tel. (+49) 251 833 9821; Fax (+49) 251 833 8388

prebodies, which are surrounded by a half-unit membrane of phospholipids.

#### Introduction

Many organisms synthesize neutral lipids as an integral part of their metabolism and as energy storage compounds. In plants, triacylglycerol (TAG) biosynthesis is mainly important for the germination of seeds (Tzen and Huang, 1992), whereas in animals TAG biosynthesis is involved in regulation of lipid concentration, milk production and fat storage in adipocytes (Murphy and Vance, 1999). In eukaryotic microorganisms, such as yeasts, TAG biosynthesis is also very common (Clausen et al., 1974; Leber et al., 1994; Sorger and Daum, 2003; Mlíčková et al., 2004). Prokaryotes are also able to accumulate lipophilic storage compounds (Ratledge, 1989); however, most frequently specialized lipids such as poly(3-hydroxybutyric acid) or other polyhydroxyalkanoic acids (PHAs) are produced (Steinbüchel, 1991). Only bacteria belonging to the actinomycetes group including Mycobacterium, Rhodococcus, Nocardia and Streptomyces accumulate large amounts of TAGs which serve as storage reservoirs for energy and carbon (Olukoshi and Packter, 1994; Alvarez et al., 2000; Alvarez and Steinbüchel, 2002). Although TAG biosynthesis is mainly restricted to these few genera, bacterial TAG biosynthesis occurs frequently in the environment, because actinomycetes are the most abundant microorganisms in soil. Furthermore, important pathogenic bacteria like Mycobacterium tuberculosis and antibiotic producing bacteria like Streptomyces coelicolor accumulate TAGs. Beside the Gram-positive bacteria mentioned above, species of the genus Acinetobacter are able to synthesize large amounts of wax esters (oxoesters of long-chain primary fatty alcohols and long-chain fatty acids) and also small amounts of TAGs (Fixter et al., 1986).

In eukaryotes TAGs are stored in cells as spherical lipid particles of 0.1–50  $\mu m$  diameter, depending on the species and cell types in which they occur. These particles are known as lipid-bodies, lipid-droplets or especially in plants as oil-bodies, oleosomes or spherosomes. The lipid particles of all eukaryotic species exhibit related and relatively simple structures. They consist of a hydrophobic core of neutral lipids, mostly TAGs and steryl esters, or wax esters in jojoba (Simmondsia chinensis), surrounded

by a phospholipid (PL) monolayer with only few species of proteins bound to the surface of the particles. In plant seeds, the most abundant class of oil body-associated proteins are oleosins, which possess a structural function (Huang, 1992; Murphy and Vance, 1999; Murphy, 2001). Perilipins, the major protein of mammalian lipid bodies are thought to play a role in the assembly of the organelle (Londos et al., 1999). In yeast, several enzymes involved in lipid metabolism, namely glycerophosphate acyltransferases, sterol methyltransferases and squalene epoxidase, were associated with the lipid-bodies (Leber et al., 1994; 1998). Although eukaryotic lipid particles were intensively investigated in the past, relatively little is known about their biogenesis, and several models for their formation have been proposed (Zweytick et al., 2000). It was suggested that the site of lipid-body assembly is a specialized subdomain of the endoplasmatic reticulum (ER) where the biosynthesis enzymes and structural proteins are most probably located. According to the most accepted model, storage lipids are accumulated between the two PL leaflets of the ER, resulting in a budding lipidbody which is surrounded by a PL monolayer directly derived from the outer ER leaflet (Napier et al., 2001).

In bacteria, TAGs and waxes are accumulated as cytoplasmic inclusions virtually surrounded by a thin boundary layer similarly to eukaryotes, as it was reported for S. coelicolor and S. lividans (Packter and Olukoshi, 1995) and for Rhodococcus opacus PD630 (Alvarez et al., 1996). Recently, a wax ester synthase/acyl-CoA:diacylglycerol acyltransferase (WS/DGAT) from Acinetobacter calcoaceticus catalysing the key steps in the biosynthesis of both storage lipids was identified (Kalscheuer and Steinbüchel, 2003). This novel type of long-chain acyl-CoA acyltransferase is not related to any other known acyltransferase including the WS of jojoba, the diacylglycerol acyltransferase families 1 and 2 in yeast, plants and animals and the PL:diacylglycerol acyltransferase in yeast and plants. A large number of WS/DGAT-related proteins were identified in the genome sequences of TAG and wax ester accumulating bacteria like M. tuberculosis, M. leprae, M. bovis, M. smegmatis and S. coelicolor, assuming that this type of enzyme is responsible for wax ester and TAG biosynthesis in all oleogenous bacteria (Daniel et al., 2004). Interestingly, previous investigations in the pathogenic *M. tuberculosis* indicated an important role of lipid accumulation in vitro and in sputum (Garton et al., 2002; Daniel et al., 2004). We are interested in the structural assembly of lipid-bodies in bacteria, with special interest in the orchestration of early stages of lipid-body formation and the mechanisms involved therein. Based on the obtained results, we developed a comprehensive model clearly distinguishing lipid-body formation in prokaryotes from the formation of similar structures in eukaryotes. Our strategy was based on the hypothesis that bacterial neutral lipids are synthesized in direct association with the cytoplasm membrane (Christensen et al., 1999; Murphy and Vance, 1999; Murphy, 2001). Furthermore, our study demonstrates that formation of wax esterand TAG-bodies in bacteria relies on the same cellular mechanisms

#### Results

Bacterial lipid accumulation is highly upregulated under conditions presenting a high carbon to nitrogen ratio

In the last few years many studies investigating the neutral lipid metabolism of bacteria, especially Acinetobacter sp. and Rhodococcus sp. were published; however, only little information is known about the time-course of neutral lipid synthesis in these bacteria. Because A. calcoaceticus ADP1 and R. opacus PD630 were most intensively investigated in the past, they were chosen as model organisms for these studies. We started our investigations with an observation of lipid accumulation as a function of time. R. opacus PD630 stored minor amounts of TAGs under conditions permitting intensive cell proliferation, whereas A. calcoaceticus ADP1 accumulated minor amounts of wax esters and very small amounts of TAGs as shown by thin layer chromatography (TLC) (Fig. 1A). In both organisms storage lipid accumulation of cells was drastically enhanced within 1 day after transferring the cells from Luria-Bertani (LB) or Standard I (Std I) complex medium to defined mineral salts medium (MSM) with a low nitrogen to carbon ratio, as revealed by TLC and gas chromatographic quantification of accumulated fatty acids (Fig. 1A and B). After 24 h of incubation in MSM, R. opacus PD630 and A. calcoaceticus ADP1 yielded total cell dry matters of 0.5 or 0.22 g l<sup>-1</sup> respectively.

Bacterial wax ester- and TAG-biosynthesis starts at the cytoplasm membrane at special lipid domains and ends in the formation of cytoplasmic lipid-bodies

Although much is known about the chemical structure of bacterial lipids, their exact localization within the cells is often unknown. An obvious problem in investigating the morphological organization of lipids is the limited availability of suitable methods sustaining the native organization of cells. Therefore, we used the fluorescent dyes Nile Red and Bodipy FL C<sub>12</sub> for the *in vivo* staining of cellular lipids. With both dyes a clear fluorescence staining of cell lipids was obtained; however, the resulting staining patterns were different. Application of the amphiphilic Bodipy FL C<sub>12</sub> to cells of A. calcoaceticus ADP1 at the beginning of lipid accumulation resulted in a selective staining of lipid domains at peripheral areas of the cells (Fig. 2A and supplemental animated Fig. S1 and S5 on Molecular

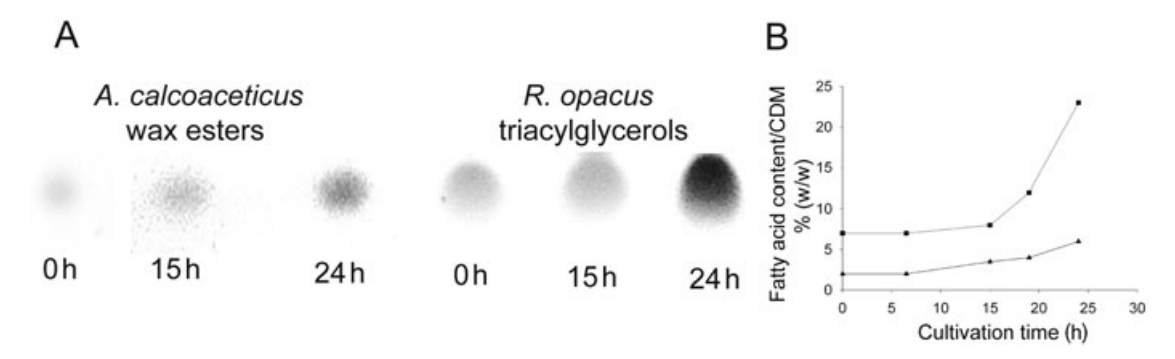


Fig. 1. Quantification of lipids in A. calcoaceticus ADP1 and R. opacus PD630.

A. Thin layer chromatograms demonstrating the increase of accumulated wax esters and TAGs in *A. calcoaceticus* ADP1 and *R. opacus* PD630 under conditions promoting lipid biosynthesis.

B. Quantification of total cellular fatty acids in both strains (▲, A. calcoaceticus; ■, R. opacus).

microbiology website). After 24 h under cultivation conditions promoting lipid accumulation, a significant increase of the expansion of these lipid domains could be demonstrated, but most of the fluorescent structures were still

located at peripheral areas of the cells (Fig. 2B and supplemental Figs. S2 and S6).

In *R. opacus* PD630 Bodipy FL C<sub>12</sub> caused also a significant staining of lipid domains at peripheral areas of the

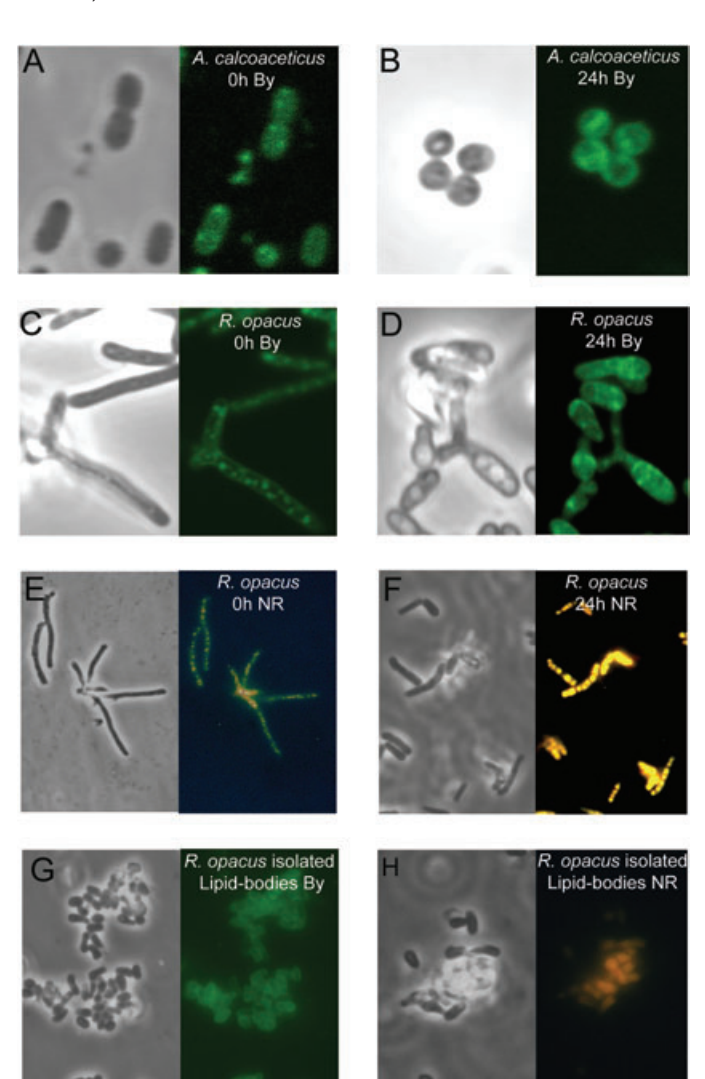


Fig. 2. Staining and localization of lipids in A. calcoaceticus ADP1 and R. opacus PD630. Phase contrast and Bodipy FL C<sub>12</sub> fluorescence micrographs of cells of A. calcoaceticus ADP1 not grown under storage conditions (A) and grown for 24 h under storage conditions (B). Phase contrast and Bodipy FL C<sub>12</sub> fluorescence micrographs of cells of R. opacus PD630 not grown under storage conditions (C) and of cells which were grown under conditions promoting lipid biosynthesis for 24 h (D). Nile Red staining of cells of R. opacus PD630 not grown under storage conditions (E) and of cells accumulating high amounts of cytoplasmic lipid-bodies after 24 h (F). Bodipy FL C<sub>12</sub> (G) and Nile Red (H) staining of isolated lipid-bodies from R. opacus PD630. Labelling of isolated lipidbodies and whole cells was performed as described in Experimental procedures. The arrows point to densely stained regions representing peripheral TAG and wax ester domains in R. opacus PD630 and A. calcoaceticus ADP1 respectively. The arrowhead indicates an intensively stained lipid-body in R. opacus PD630. By, Bodipy FL C<sub>12</sub>; NR, Nile Red.

cells when lipid accumulation started, with also a clear staining of cell wall structures (Fig. 2C and Figs. S3 and S7). In phase-contrast microscopy, these inclusions appeared as dark and small granules in R. opacus PD630 like in A. calcoaceticus ADP1. After prolonged lipid accumulation, R. opacus PD630 cells exhibited a faint, superficial fluorescence which was associated with large inclusion bodies in the cytoplasm and a strong staining of peripheral lipid domains, similar to that in the earlier stage. At this time large lipid-bodies were clearly located in the central part of the cytoplasm and were filling almost the whole cell, as represented by the large, light scattering particles in phase contrast micrographs (Fig. 2D and Figs S4 and S8).

Using the lipophilic dye Nile Red in R. opacus PD630 at an early stage of lipid biosynthesis, small lipid domains were observed in the cells, which were predominantly located at peripheral areas of the cells (Fig. 2E). This corresponded to the findings obtained with Bodipy FL C<sub>12</sub>-stained cells from the same accumulation stage. In contrast to Bodipy FL C12, Nile Red staining resulted in an exclusive staining of large cytoplasmic lipid-bodies in R. opacus PD630 after 24 h, without any staining of cell wall components (Fig. 2F). These different staining properties of Bodipy FL C12 and Nile Red were also observed in vitro during staining of matured lipid-bodies from R. opacus PD630 (Fig 2G and H). Nile Red imbues the whole lipid matrix of the lipid-bodies because of its throughout lipophilic character, whereas the Bodipy FL C<sub>12</sub> fluorophore cannot reach deeper areas of the lipid-bodies because of its hydrophilic carboxy group, explaining the different fluorescence patterns.

# Lipid-bodies are formed from lipid-prebodies and an oleogenous layer at the cytoplasm membrane

Application of fluorescent dyes in this study on lipid-body biogenesis indicated that prokaryotic neutral lipid accumulation was initiated at the cytoplasm membrane and that free cytoplasmic lipid-bodies occurred only at a later stage. To obtain further support for this observation, we performed transmission electron microscopic (TEM) investigations on ultra thin sections of cells from different stages of lipid accumulation. R. opacus PD630 cells exhibited a significant change in morphology during 19 h of growth under cultivation conditions promoting neutral lipid accumulation (Fig. 3A). Cells grown in complex media generally showed no or only unfrequently lipidbodies in the cytoplasm (data not shown). After 6.5 h cultivation under storage conditions, flat to spherical, relatively electron-dense structures close to the cytoplasm membrane were observed. These structures were referred to as lipid-prebodies. These lipid-prebodies did

not show a clearly visible boundary layer, and the material they were consisting of, was distributed over the whole cytoplasm membrane at an uneven thickness. This layer was referred to as oleogenous layer. The distribution of the lipid-prebodies was similar to that of peripheral lipid domains as observed in fluorescence and phase contrast microscopy. These spherical lipid-prebodies enlarged further to an average diameter of about 300 nm, followed by an apparent dissociation from the oleogenous layer resulting in their release into the cytoplasm. Interestingly, these lipid-prebodies showed a wide variety of electron density, from a diffuse shape, which could be only hardly distinguished from the cytoplasm, to a clearly visible, nearly opaque shape. Already after 15 h cultivation, the cytoplasm was almost completely filled with large, electron opaque lipid-bodies with an average diameter of 400-600 nm and with an implied boundary layer and no visible contact to the cytoplasm membrane. However, lipid-prebodies were observed at much lower levels, and finally disappeared after 19 h cultivation. At this stage, cells were fully enriched with cytoplasmic lipid-bodies, which also sporadically coalesced with each other.

In A. calcoaceticus ADP1 the formation of wax-bodies originated also close to the cytoplasm membrane. However, differentiation between wax-prebodies and matured wax-bodies was more difficult: these inclusions exhibited a clear electron opaque shape already at the beginning of their formation because they were more clearly separated from the cytoplasm as compared to the much more diffuse lipid-prebodies in R. opacus PD630 (Fig. 3B). These membrane bound wax-prebodies were also in direct conjunction with an oleogenous layer at the surface of the cytoplasm membrane similar to that observed in R. opacus PD630; however, this layer exhibited a lesser extension. The black precipitate inside the lipid-prebodies of R. opacus PD630 noticed after DAB photoconversion of Bodipy FL C<sub>12</sub>-stained cells in transmission electron micrographs revealed that these structures contained stained lipids and corresponded to the observed peripheral lipid domains in fluorescence microscopy (Fig. 3C). In both organisms, membrane splitting, which would indicate lipid accumulation between the two leaflets of the cytoplasm membrane like in the eukaryotic ER model, did never occur. The membranes stayed visibly intact in all performed TEM preparations (see Fig. 3B as an example).

## WS/DGAT is localized at the bacterial cytoplasm membrane

We used polyclonal anti-WS/DGAT IgGs for immunogold localization of this enzyme in A. calcoaceticus ADP1 at a growth stage when lipid accumulation was just starting.

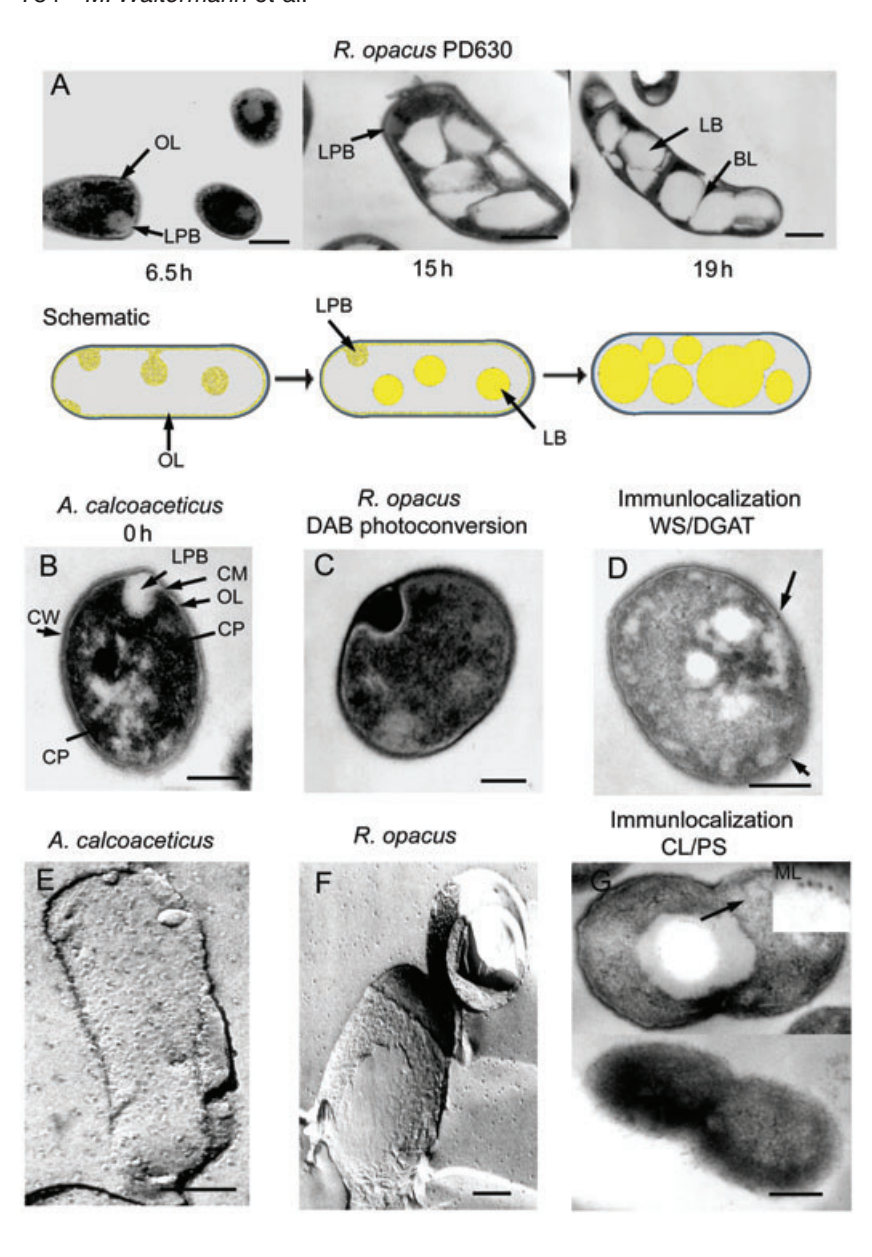


**Fig. 3.** Morphological and immunological characterization of lipid-body formation in *R. opacus* PD630 and *A. calcoaceticus* ADP1.

A. TEM micrographs and scheme of cells of R. opacus PD630 grown under storage conditions for 6.5, 15 and 19 h.

B. Image shows a cell of *A. calcoaceticus* ADP1 not grown under storage conditions with a nascent wax ester-body originating from the cytoplasm membrane.

C. DAB photoconversion of a Bodipy FL  $C_{12}$ -labelled cell of R. opacus PD630 represents a dark precipitate inside one lipid-prebody.

D. A. calcoaceticus ADP1 labelled with rabbit anti-WS/DGAT IgGs and goat anti-rabbit IgGs loaded with 10 nm colloidal gold (arrows on black dots).

E, F. Freeze fracture preparations of (E) A. calcoaceticus ADP1 and (F) R. opacus PD630, exhibiting wax ester prebodies and a matured, cytoplasm localized TAG-body respectively.

G. Immunlocalization of CL and PS with monoclonal human anti-CL/PS IgGs in *A. calcoaceticus* ADP1 and goat anti-human IgGs loaded with 5 nm colloidal gold (arrows on black dots).

Scale bars = 0.2  $\mu$ m. BL, boundary layer; CM, cytoplasm membrane; CP, cytoplasm; CW, cell wall; LB, lipid-body; LPB, lipid-prebody; ML, PL monolayer; OL, oleogenous layer.

Ultrathin sections treated with these antibodies showed labelling at and close to the cytoplasm membrane (Fig. 3D). Statistical analysis of 50 electron micrographs, each containing one single cell, revealed between one and five labels per cell membrane region, whereas labelling of the cytoplasm and of the surface of lipid-bodies occurred at a one magnitude lower frequency, thus demonstrating that WS/DGAT was localized at the cytoplasm membrane. An increase in the concentration of the primary antibody did not result in a significant increase of specific labelling, whereas the background labelling increased clearly, indicating that only very low copies of the enzyme were present in the cells. No specific labelling was obtained in experiments using the preimmune serum (data not shown).

Lipid-bodies are surrounded by a half-unit membrane of phospholipids

Freeze-fracture is a suitable tool for analysis of PL-membranes. A frozen membrane splits along its hydrophobic core resulting in an interior view of the membrane at the fracture faces. The P-face is defined as the fracture face of the cytoplasmic (protoplasmic) leaflet of the membrane, whereas the E-face means the fracture face of the extracellular leaflet. In freeze-fracture preparations of *A. calcoaceticus* ADP1 wax-prebodies were localized at the peripheral areas of the cells, confirming previous experiments described above (Fig. 3E). In contrast, lipid-prebodies could not be detected in the respective preparations of *R. opacus* PD630; however, matured lipid-

bodies with a lamellar internal structure were observed, as recently described for lipid-bodies in cultured smooth muscle cells (Fig. 3F) (Robenek et al., 2004). For this reason, the standard freeze-fracture nomenclature cannot be applied to prokaryotic lipid-bodies, as these inclusions do not have a PL-bilayer structure at the surface which delineates a true lumen. Furthermore, referring to the lamellar internal structure of lipid-bodies in freeze-fracture preparations, it is difficult to ascertain whether one is dealing with a true outer PL layer or an adjacent underlaying lipid layer, because freeze-fracturing splits the hydrophobic planes between these layers at various depths through the lipid-body core yielding lamellar views similar to that of membrane fracture faces. For this reason we performed an immunlocalization experiment using human monoclonal IgGs raised against cardiolipin (CL) and phosphatidylserine (PS) from a patient suffering anti-PL syndrome to discover the distribution of these PLs in situ (Lackner et al., 2000). Ultrathin sections of A. calcoaceticus ADP1 showed only a sparing PLlabelling at the cytoplasm membrane and outer membrane of cells which were fully embedded in the polymeric resin. Only cells which had partly detached from the resin, showed an intensive labelling of the outer membrane PL, which is due to the greater surface accessible for the antibody. However, the surfaces of lipid-bodies were intensively labelled, because most of the lipids contained therein were extracted previously by the dehydration process exposing the remaining surrounding PLs to the antibody (both images in Fig. 3G).

# Formation of membrane-bound lipid-prebodies and free lipid-prebodies can be performed in vitro

To circumstantiate our observations in bacterial lipid-body biogenesis described above, we constructed an artificial system for the formation of lipid-bodies and measurement of their mass increase. First, the in vitro adsorption of WS/ DGAT from A. calcoaceticus ADP1 to an artificial bacterial membrane was investigated by means of a quartz crystal microbalance (QCM) (Sauerbrey, 1959; Muratsugu et al., 1993; Janshoff et al., 2000). This technique is a versatile method for in situ quantification of protein and lipid adsorption on functionalized surfaces. At first, the time course of WS/DGAT attachment to a model membrane was studied. The shift in resonance frequency of the quartz resonator after adsorption of WS/DGAT at the resonator bound PL membrane with a final concentration of 30 μg ml<sup>-1</sup> is shown in Fig. 4A. The adsorption of WS/ DGAT occurred as a two step process consisting of two individual exponential curves of decreasing resonance frequency within an adsorption time of about 30 min before reaching a new steady state at the end of the second adsorption step. The first step took only several

minutes and was proportional to the amount of enzyme used in the respective assay (data not shown). Partially overlapping with the first adsorption step, a second step followed in which soluble and membrane-bound enzyme reached equilibrium after an observed total frequency shift of  $\Delta_f = 40 \pm 5$  Hz. Thereafter, the frequency shifts of quartz resonators were recorded after starting the reactions catalysed by WS/DGAT by adding palmitoyl-CoA and an acceptor molecule like hexadecanol or 1,2dipalmitoylglycerol, resulting in the formation of wax esters or TAGs, thus proving synthesis and accumulation of neutral lipids at the artificial PL membrane. The response of the quartz crystal after washing the QCM chamber with fresh buffer to eliminate unbound enzyme was first monitored after addition of palmitoyl-CoA and hexadecanol. The addition of the substrates resulted in an exponential decrease of the resonance frequency for a period of 180 min, with a total frequency shift of  $\Delta_f = 70 \text{ Hz}$ (Fig. 4B). The observed frequency shift was in direct relation to the amount of synthesized wax ester, as was shown in different experiments varying in the amounts of added palmitoyl-CoA (Fig. 4C). The frequency shift was observed only in experiments with all components added required for wax ester biosynthesis, such as WS/DGAT, palmitoyl-CoA and hexadecanol, whereas no frequency shift was observed in control experiments lacking one of these components (data not shown). Similar results were obtained in experiments using 1,2-dipalmitoylglycerol as an acyl acceptor, resulting in the formation of TAGs (Fig. 4D). Even in experiments using ethanol as a water soluble acyl acceptor forming palmitoylethyl ester, lipid formation occurred on the artificial PL membrane (Fig. 3E) (T. Stöveken, R. Kalscheuer and A. Steinbüchel, submitted; Kalscheuer et al., 2004). In all experiments performed overnight a slow but clear increase of resonance frequency occurred after the enzyme reaction has finished. This increase reached a new steady state after approximately 10 h and exceeded not the initial resonance frequency  $f_s$  of the quartz after enzyme adsorption, which is a clear hint for the formation of lipid-prebodies and their slow dissociation from the enzyme bound to the artificial PL membrane (Fig. 4F).

# Lipid-prebodies are conglomerates of small lipid droplets (SLDs)

The results of the QCM experiments clearly demonstrated the formation and accumulation of neutral lipids on the artificial bacterial PL membrane resulting from WS/DGAT activity. However, the shape of lipids accumulated on the membrane and the formation of putative artificial lipidprebodies were not shown in detail by the QCM method. Therefore, we investigated the formation of small wax ester droplets and their conglomeration and coalescence

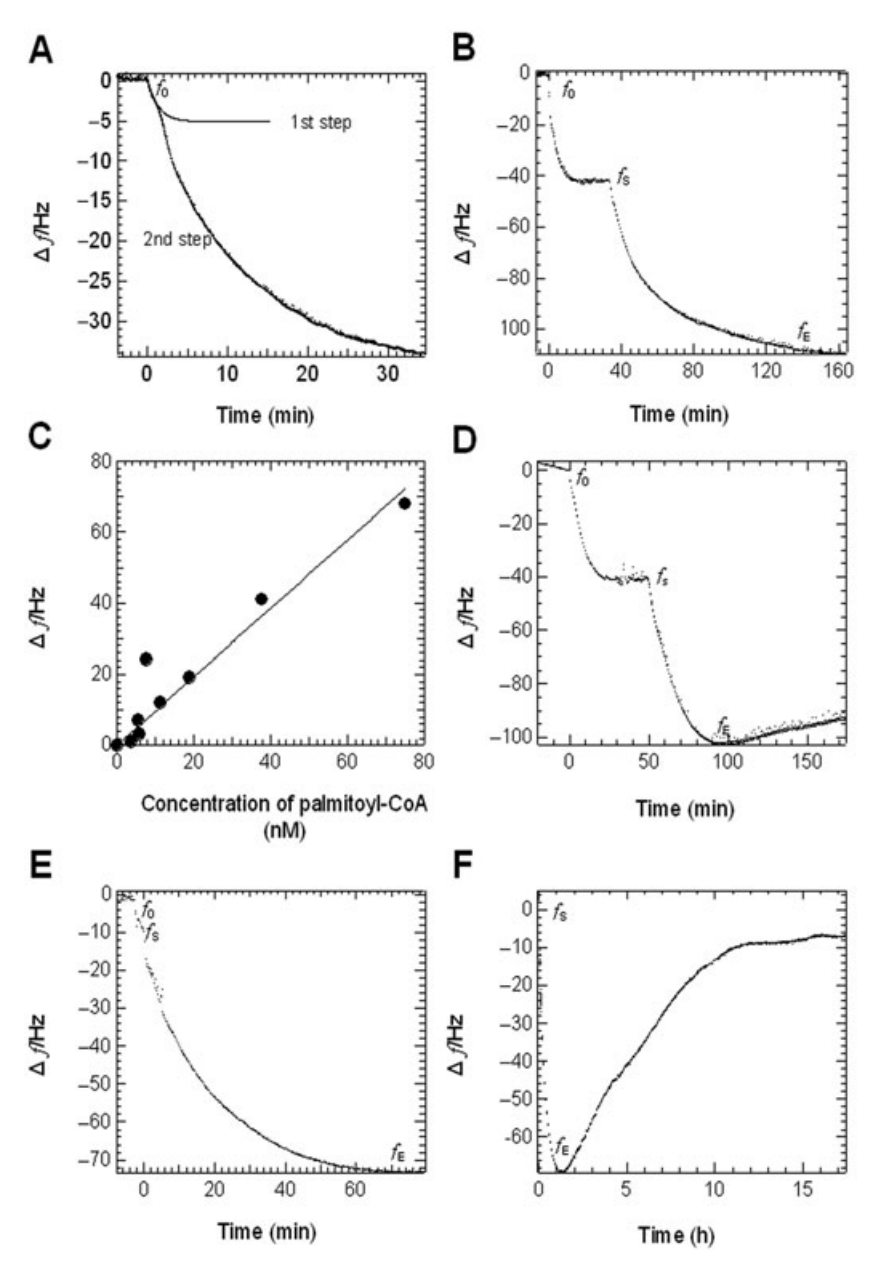


**Fig. 4.** Quartz crystal microbalance measurements of WS/DGAT adsorption and activity *in vitro*.

A. Two-step adsorption of WS/DGAT on a solid phase-supported artificial membrane. The first exponential step in decrease of resonance frequency is drawn as a continuous line. Formation of wax esters (B),TAGs (D) and ethylpalmitoyl esters (E) on solid phase-supported artificial membranes.

C. The dependence of the observed total frequency shift on the concentration of palmitoyl-CoA added to the respective WS/DGAT assay during *in vitro* wax ester biosynthesis. After WS/DGAT has lost activity, artificial wax esters dis-

quency shift on the concentration of palmitoyl-CoA added to the respective WS/DGAT assay during *in vitro* wax ester biosynthesis. After WS/DGAT has lost activity, artificial wax esters dissociate slowly from the membrane as shown in an overnight experiment (F). Immediately after the enzymatic reaction has stopped, the resonance frequency of the quartz crystal slowly increases and reaches a new steady state near  $f_0$ . Abbreviations for resonance frequencies:  $f_0$ , frequency before incubation with WS/DGAT;  $f_0$ , before addition of substrates; and  $f_0$ , at the end of the enzymatic reaction.

to lipid-prebodies on mica sheets instead of a quartz resonator, which were topographically scanned by scanning force microscopy (SFM). In these experiments direct adsorption of the enzyme was not observed because of the low resolution of the experimental setup. Similar to the QCM experiments, changes of the surface topography after addition of palmitoyl-CoA and hexadecanol to the membrane bound WS/DGAT were monitored. During the time-course of the experiments drastic changes in the surface topography of the mica sheets occurred. Immediately after addition of the substrates droplet-like structures were formed at the surface of the mica sheets, resulting in mountainlike structures all over the scanned area of the sheets during the first 90 min (see Fig. 5A and B for con-

tact mode images). These droplet-like structures showed an average diameter of about 50 nm and an average height of 15 nm and were referred to as small lipid droplets (SLDs). Most probably, these droplet-like structures represented the basal unit from which lipid-prebodies and cytoplasmic lipid-bodies were formed *in vivo* and which formed the oleogenous layer at the cytoplasm membranes as shown by TEM investigations. Each of these SLDs was probably the result of the biosynthetic activity of only one single WS/DGAT enzyme. After additional 60 min, many of the SLDs had conglomerated or coalesced with adjacent SLDs forming large, spherical structures (see Fig. 5C for an image in tapping mode). These larger spherical structures exhibited diameters of more than 300 nm and

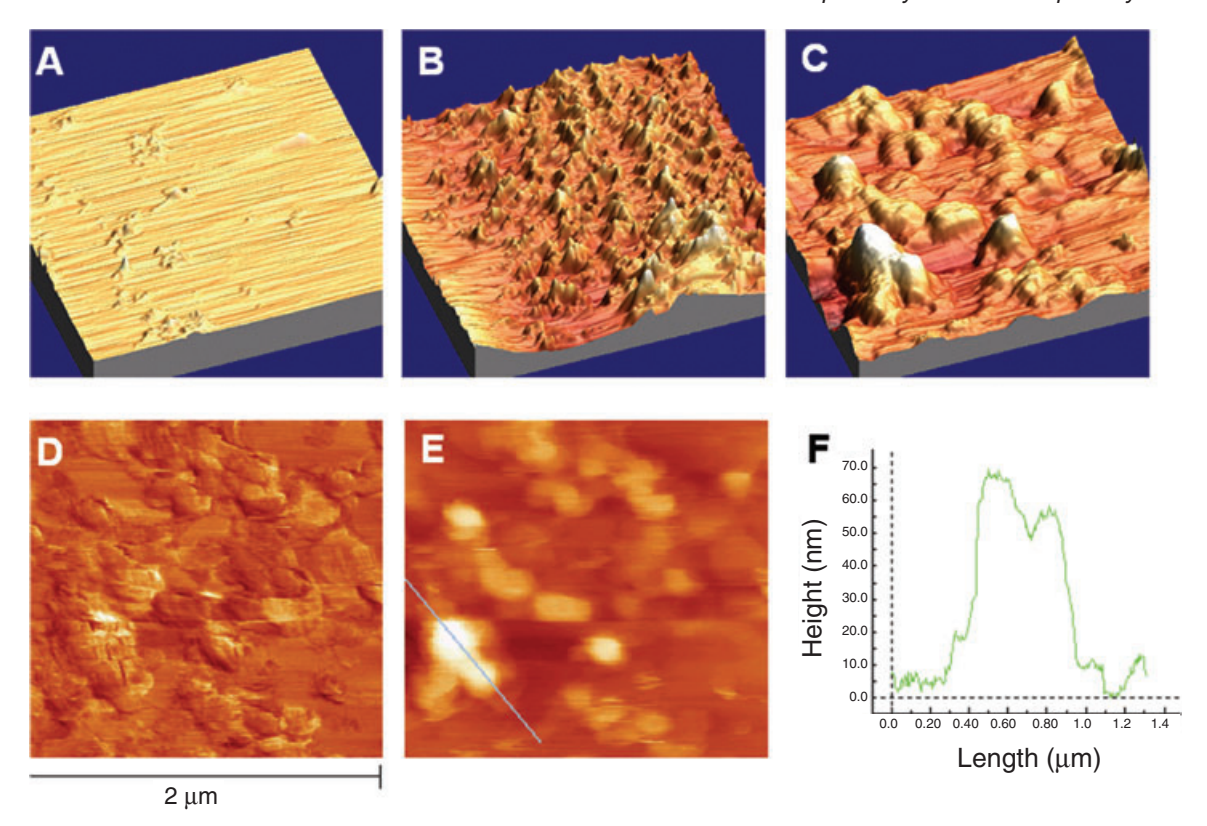


Fig. 5. Formation of SLDs and lipid-prebodies on a solid phase-supported PL membrane as revealed by scanning force microscopy. Change in surface topography of a mica sheet because of WS/DGAT activity on a solid phase-supported artificial membrane (A) 0 min, (B) 90 min and (C)150 min after addition of palmitoyl-CoA and hexadecanol. Scans (A) and (B) were recorded in contact-, scan (C) in tapping mode. (D) represents the phase signal and (E) the height signal of scan (C). (F) represents a height profile indicated by the bar in (E) crossing two artificial lipidprebodies.

an average height of about 70 nm (Fig. 5D-F); thereby representing a comparable or even greater dimension and volume as the lipid-prebodies visible in the transmission electron micrographs.

#### Discussion

Acinetobacter calcoaceticus ADP1 and R. opacus PD630 represent two model organisms for bacterial wax esterand TAG-biosynthesis. In both organisms neutral lipids are finally deposited as insoluble intracytoplasmic lipidbodies. The results presented in this study revealed the fundamental mechanisms in the formation of these lipidbodies in bacteria (Fig. 6A). The fluorescence staining experiments showed that lipid biosynthesis starts at peripheral lipid domains close to the cytoplasm membrane previously shown by Christensen et al. (1999). Later, further biosynthesis of lipids led to the formation of large, spherical, cytoplasm-localized lipid-bodies (Packter and Olukoshi, 1995; Alvarez et al., 1996). The phases of lipid accumulation were implicated to structures in TEM preparations, starting with an oleogenous layer at the cytoplasm membrane and the subsequent formation of lipid-prebodies. The latter are then released into the cytoplasm after reaching a critical size, and matured lipidbodies are formed.

At the beginning of this study it was unexplainable how an oleogenous layer could surround the cytoplasm membrane, because a complete coating of the membrane with confluent lipids would prevent most membrane-associated metabolic processes of the cell. The only explanation of this phenomenon was the occurrence of an immobilized lipid emulsion, initially consisting of non-confluent SLDs synthesized by the WS/DGAT, which was finally confirmed by the SFM experiments. Most probably SLDs remain in this stage associated with WS/DGAT because of hydrophobic interactions between the enzyme and the synthesized lipids. Hydrophilic regions between these SLDs would allow normal metabolic processes, such as lipid biosynthesis itself. This growing SLD emulsion is rather unstable, and therefore, the SLDs accumulate at certain parts of the cell to form the observed lipid-prebodies. These lipid-prebodies were thought to consist of an SLD emulsion growing until a critical diameter is reached, i.e. of about 300 nm in R. opacus. The emulsion like composition of the oleogenous layer and the lipid-prebodies

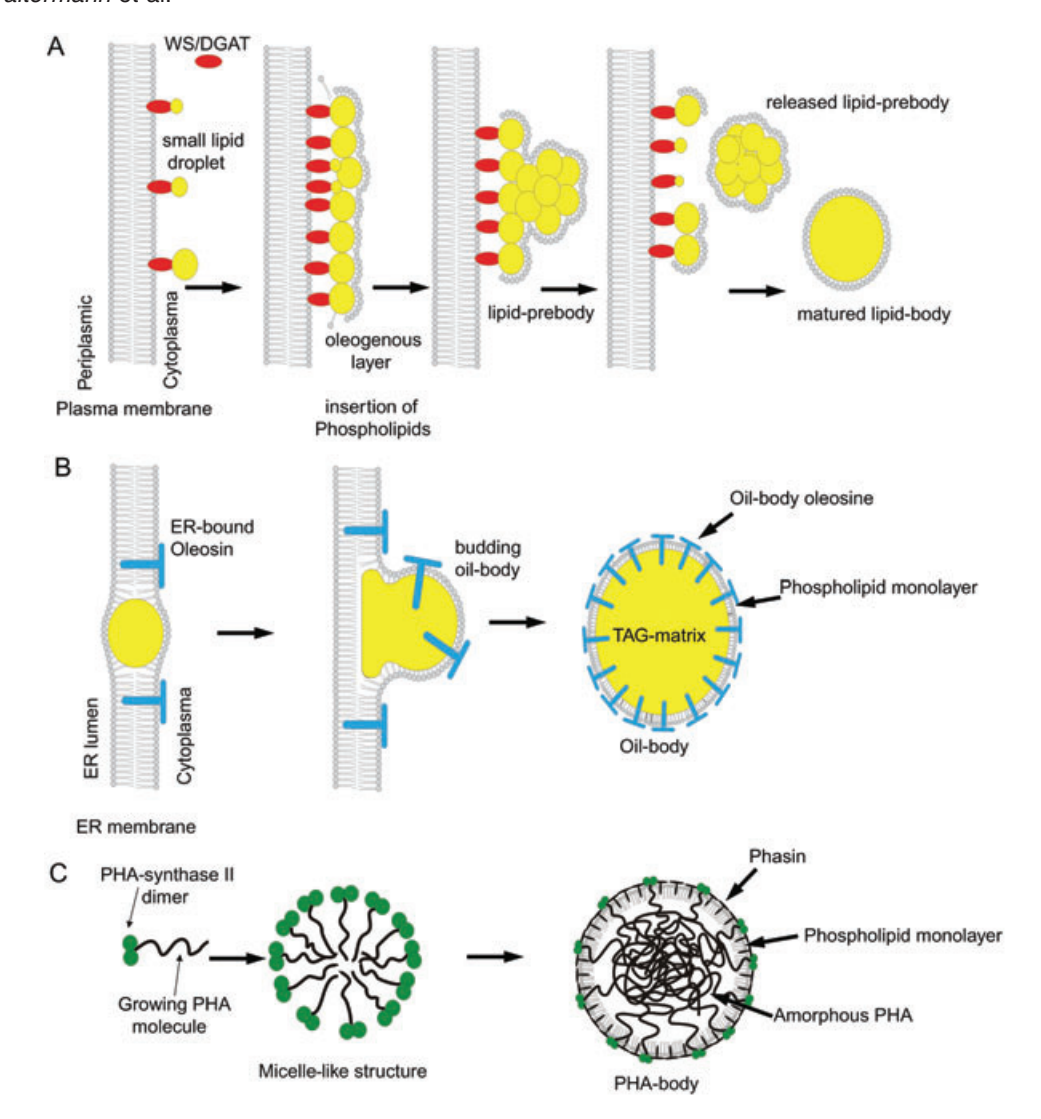


Fig. 6. Models proposed for lipid-body formation in prokaryotes and eukaryotes.

A. Prokaryotic TAG- and wax ester-body formation. In prokaryotes neutral lipid-body formation starts with attachment of WS/DGAT to the cytoplasm membrane and subsequent synthesis of SLDs forming an oleogenous layer, which is coated by a monolayer of PLs. Lipid-prebodies are formed by conglomeration and coalescence of SLDs leading to the formation of membrane bound lipid-prebodies and afterwards cytoplasmic lipid-bodies. B. Oil-body formation in plant seeds. Eukaryotic oil-bodies are formed by progressive accumulation of lipids between the two leaflets of the ER membrane with a possible co-translational insertion of structural proteins (e.g. oleosins in plant seeds), resulting in a budding oil-body which is released into the cytoplasm.

C. Prokaryotic PHA-body formation. Prokaryotic PHA-bodies are synthesized by the formation of cytoplasmic, micelle-like structures from primed PHA-synthase and the newly synthesized PHA-chain. Progressive PHA-biosynthesis leads to a growing PHA-body in which structural proteins (phasins) and PL are inserted. Please note that not all components contributing to the various lipid-bodies could be drawn at their true scale.

caused probably the granulous shape of these structures in TEM preparations. However, SLDs have to be temporarily stabilized before they undergo controlled coalescence in lipid-prebodies. It is possible that unspecific interactions with proteins of the cytoplasm cause a temporary stabilizing effect of this emulsion. This is indicated by the high amounts of unspecifically bound proteins on isolated lipid-bodies. It is also possible that SLDs are more or less coated by PLs, and that the progressing coalescence is moreover driven by a migration of the PLs to the

surface of lipid-prebodies. The subcellular localization of WS/DGAT in *A. calcoaceticus* ADP1 using immunogold techniques clearly demonstrated that this enzyme is mostly membrane-bound *in vivo*. It was demonstrated that WS/DGAT is most probable associated to the cytoplasm membrane by ionic interactions, rather than by an integral conformation (T. Stöveken, R. Kalscheuer and A. Steinbüchel, submitted). The only evident localization for TAG-and wax ester-biosynthesis is the cytoplasm membrane, because most of the enzymes, which are involved in lipid

biosynthesis and in replenishment of substrates, are compartmented between the cytoplasm and the cytoplasm membrane (Coleman, 1990; Reiser and Sommerville, 1997; Wilkinson and Bell, 1997). It is not clear whether the WS/DGAT stays attached to the dissociating SLDs or if it remains bound to the membrane; however, the QCM experiments suggested that WS/DGAT, once associated, remains bound at the cytoplasm membrane after dissociation of SLDs and lipid-prebodies. However, some enzymes remain probably also attached to the lipid-prebodies during the dissociation process and are therefore later localized on matured lipid-bodies, as was shown by T. Stöveken, R. Kalscheuer and A. Steinbüchel, (submitted).

Furthermore, it was demonstrated that matured lipidbodies were at least partially surrounded by a half-unit membrane of PLs, and it is very likely that PLs come already in close contact to membrane-bound SLDs, because otherwise it could not be explained how PLs are targeted to lipid-bodies inside the cytoplasm. It is very likely that PLs play a major role in the formation and control of prokaryotic lipid-bodies and their stability. Indeed, visualization of SLDs in TAG and wax ester accumulating, living cells is nearly impossible, but we provided an in vitro simulation by employing QCM and SFM to investigate the formation of SLDs and lipid-prebodies in the first phases of lipid-body formation. The artificial lipidprebodies grew to a volume comparable to those observed by TEM preparations, and left the solid phasesupported PL membrane after the enzyme lost activity. It is possible that the absence of free PLs in our experiments caused the relatively flat shape of these structures observed by SFM, although nascent lipid-prebodies also showed a flat shape in TEM preparations. The occurrence of a water-permeable SLD emulsion is also confirmed by the selective staining of lipid-prebodies with Bodipy FL C<sub>12</sub> in contrast to the superficial staining of matured lipidbodies with this dye. The complete staining of lipid-prebodies would only be possible if the dye reaches a great surface within these structures, which is surrounded by the cytoplasm. It is very likely that matured lipid-bodies are formed from lipid-prebodies simply by progressive coalescence of the SLDs leading to a homogenous and compact lipid core causing its opaque shape in TEM.

In the past, we tried to identify structural proteins specifically bound to the surface of isolated lipid-bodies (Kalscheuer et al., 2001). However, even all strongly associated proteins found in isolated lipid-bodies could not be related to the lipid-bodies indicating that these proteins became bound to the lipid-body surface only during cell disruption (M. Wällermann and A. Steinbüchel, unpubl. results). Thus, bacterial lipid-bodies are most likely comparable to lipid-bodies in yeast or the mesocarp tissue from olive or avocado, which are also completely lacking

structural proteins (Murphy and Vance, 1999; Murphy, 2001). Nevertheless, this assumption does not eliminate the possibility that specific proteins with metabolic functions, for example, lipases involved in lipid mobilization, are bound to the surface of lipid-bodies, similar to the situation observed in yeast (Murphy and Vance, 1999; Murphy, 2001). However, the difficulties in preparing native bacterial lipid-bodies demand for non-invasive in situ studies to reveal their true protein composition in future. Despite this structural analogy, plant lipid-body formation is quite different. Plant lipid-bodies are thought to arise from the ER by an accumulation of lipids between the two leaflets of the ER and where structural proteins like the oleosins are inserted (Fig. 6B) (Murphy and Vance, 1999; Murphy, 2001). Furthermore, bacterial neutral lipid-bodies must be clearly distinguished from PHA inclusions with respect to their formation. It is believed that PHA inclusions are formed from primed dimeric PHAsynthases, which form micellar structures with the growing PHA-chains. In this model, phasins and PLs are targeted to the growing PHA inclusion (Fig. 6C) (Stubbe and Tian, 2003; Jurasek and Marchessault, 2004; Pötter et al., 2004). PHA inclusion formation through budding from the cytoplasm membrane was only recently discussed as a possible alternative (Stubbe and Tian, 2003).

#### **Experimental procedures**

#### Strains and culture conditions

Cells of A. calcoaceticus ADP1 (ATCC 33305) were cultivated aerobically in LB medium (Sambrook et al., 1989) in Erlenmeyer flasks at 30°C, whereas cells of R. opacus PD630 (DSM 44193, Alvarez et al., 1996) were grown in Standard I (Std I) medium (Merck, Germany) under the same conditions. These conditions were referred to as growth conditions. To promote wax ester- and TAG-biosynthesis, cells of A. calcoaceticus were cultivated for 6.5, 15, 19 and 24 h in MSM (Schlegel et al., 1961) with 0.1 g l-1 NH<sub>4</sub>Cl and with  $10 \ g \ l^{-1}$  glucose as carbon source (storage conditions). R. opacus PD630 was cultivated under the same conditions except that 10 g l-1 sodium gluconate were used as carbon source instead of glucose.

## Purification of lipid-bodies

Lipid-bodies from R. opacus PD630 were purified from crude cell extracts in a discontinuous glycerol density gradient as described previously (Kalscheuer et al., 2001).

#### Fluorescence labelling of cells

For fluorescence labelling, DMSO stock solutions (0.5 mg ml<sup>-1</sup>) of Bodipy FL C<sub>12</sub> (Molecular Probes, USA) and Nile Red (Sigma, Germany) were diluted to  $0.5\,\mu g\ ml^{-1}$  with PBS (0.9% NaCl [w/v], 0.1 M, pH 7.5). Cell suspensions (1000 μl) were harvested by centrifugation at 13 000 r.p.m. for 5 min, and cells were resuspended in the same volume of staining buffer and incubated for 30 min on ice in the dark. After staining, the cells were washed three times with PBS and were used immediately for phase contrast and confocal laser scanning microscopy.

#### Confocal laser scanning microscopy

Confocal optical sectioning was performed with a Leica TCS2 confocal laser scanning system (Leica TCS SP2, Leica Mikrosysteme, Germany). A Krypton/Argon laser with an excitation wavelength of 488 nm was used to activate the fluorescence of Bodipy FL  $C_{12}$  and Nile Red. Optical sections were collected throughout the entire stained cell preparation with a Z-step interval of  $0.1-0.2~\mu m$ . The clearest images were obtained by using an average Kalman filtering of four times. High magnification images were obtained with a  $63\times$  objective lens with oil immersion. To minimize fluorescence bleaching during scanning, low laser light source intensity was applied.

# Transmission electron microscopy (TEM) and immunogold labelling

The cells were fixed with 2.5% (w/v) glutaraldehyde in 0.1 M PBS (pH 7.3) for 16 h according to Sørensen (Arnold, 1968) after washing three times in PBS (pH 7.3). After three washing steps in PBS each for 20 min, the cells were postfixed employing 1% (w/v) osmium tetroxide in 0.1 M PBS (pH 7.3) for 90 min and washed once with PBS for 15 min. Then the water was removed by a graded water-ethanol series (30%, 50%, 70%, 90%, 96% and 100% ethanol) each step for 15 min. For thin sectioning, the samples were embedded in SPURR resin (Spurr, 1969) with 50% (w/v) propylene oxide for 4 h and resin with 33% (w/v) propylene oxide for 16 h. The SPURR resin was changed every 24 h for a period of 3 days. The polymerization of the resin was performed at 70°C for 48 h. Sections with a thickness of 70-80 nm were made with an Ultracut Microtome (LEICA Mikroskopie und Systeme GmbH, Germany) using a diamond knife and were subsequently placed on a 200 mesh copper grid. Imaging was performed with a H-500 TEM (Hitachi, Japan) in the bright-field mode at 75 kV acceleration voltage at room temperature. For immunogold labelling, cells of A. calcoaceticus ADP1 were fixed for 16 h in 300 mM PIPES, pH 7.3, containing 6% (w/v) paraformaldehyde. Then, cells were washed three times in 300 mM PIPES, pH 7.3, and dehydrated in a graded ethanol series as was described above. For thin sectioning, the samples were embedded in a series of 33%, 50%, 66% and 100% (w/v) lowicryl resin (Polyscience, Germany) in ethanol, each step for 8 h at a temperature of 4°C. Polymerization of the resin was performed under UV light for 48 h at 35°C and for 48 h at room temperature. Preparation of thin sections was performed as described above.

For immunogold labelling ultrathin sections were applied on nickel grids and incubated with the following solutions: (i) rabbit anti-WS/DGAT (T. Stöveken, R. Kalscheuer and A. Steinbüchel, submitted) or HL5-B human anti-CL/PS IgG

(Lackner *et al.*, 2000), diluted 1:1–1:250 in 5% (w/v) BSA in PBS, pH 7.4, 2 h; (ii) washing in PBS, 5 min, three times each; (iii) washing 5 min in 5% (w/v) BSA in Tris/HCl, pH 8.2; (iv) goat anti-rabbit or goat anti-human IgG coupled with colloidal gold, particle size 10 or 5 nm respectively (Sigma, Germany), diluted 1:10 in BSA-Tris/HCl pH 7.4, 1 h; (v) 5 min washing in BSA-Tris/HCl pH 7.5, five times each. After labelling, sections were stained for 5 min in 0.66% (w/v) uranyl acetate and for 10 s in 0.9% (w/v) lead citrate, and finally washed in water.

#### Freeze-fracture electron microscopy

About 5 g of wet cells were harvested by centrifugation and resuspended in 30% (w/v) glycerol. The cells were snapfrozen without prior fixation in Freon 22 cooled with liquid nitrogen and freeze-fractured in a BAF310 freeze-fracture unit (Balzer AG, Lichtenstein) at  $-100^{\circ}\text{C}$  and  $2\times10^{-6}$  m bar. Replicas of the freshly fractured cells were immediately made by electron beam evaporation of platinum-carbon and carbon at angles of 38° and 90° and to thicknesses of 2 nm and 20 nm. After preparation, the replicas were photographed in a Philips 410LS electron microscope.

#### 3,3'-Diaminobenzidine (DAB) photoconversion

Diaminobenzidine photoconversion was performed according to Dantuma et al. (1998). For DAB photoconversion cells were stained with Bodipy FL C<sub>12</sub> as described above. Stained cells were washed three times in PBS and subsequently fixed for 3 days in 2% (w/v) paraformaldehyde and 0.5% (w/v) glutaraldehyde in PBS at 4°C, and rinsed again three times in PBS for 10 min before cells were embedded in 3.5% (w/v) agarose. Sections of about 200 nm were cut with a razor blade from agarose pills and incubated overnight in 2% (w/v) paraformaldehyde in PBS. After washing three times in PBS, sections were preincubated in prechilled (0°C) 0.5 mg ml<sup>-1</sup> DAB in PBS for 30 min. Preincubated sections were photo-converted for 1.5 h using a conventional fluorescence microscope (Leitz Laborlux, Germany) with a fluorescein filter setting (Leitz, BP530-560), a 50 W mercury lamp and a 10x objective. Every 15 min fresh prechilled PBS containing 0.5 mg ml<sup>-1</sup> DAB was added. The illuminated area of the agarose sections, which could be recognized by the dark DAB product, were excised and rinsed three times for 10 min, before they were postfixed for 30 min in 1% (w/v) OsO4 in PBS. Fixed sections were again washed in PBS and used for TEM preparation as described above.

# Lipid analysis

For qualitative and quantitative determination of fatty acids 5–7.5 mg of lyophilized cells were subjected for 5 h and 100°C to methanolysis in the presence of 15% (v/v) sulphuric acid in methanol. The resulting methylesters of fatty acids were analysed by gas chromatography according to Kalscheuer *et al.* (2004). Thin layer chromatography was performed as described previously (Wältermann *et al.*, 2000).

#### Vesicle preparation

Vesicles were prepared from mixtures of dipalmitoylphosphatidylcholine (DPPC), dipalmitoylphosphatidylglycerol (DPPG), CL and dipalmitoylphosphatidylserine (DPPS) in a molar ratio of 75:18:5:2. Mixed lipid films were prepared by dissolving lipids in chloroform/methanol 1:1 (v/v) and afterwards drying under a stream of nitrogen while heating above the main phase transition temperature  $T_{\mathrm{m}}$ . Remaining solvents were evaporated for 2 h under vacuum. Multilamellar vesicles were prepared by swelling and resuspending the lipid films in buffer solution (140 mM NaCl, 2.7 mM KCl, 8.1 mM Na<sub>2</sub>HPO<sub>4</sub>, 1.5 mM KH<sub>2</sub>PO<sub>4</sub>, pH 7.4) while heating above  $T_{\rm m}$  and vortexing periodically three times for 30 s. The resulting multilamellar vesicles were subsequently sonicated for 15 min in a water bath to get large unilamellar vesicles (LUVs).

# Surface functionalization and guartz crystal microbalance (QCM) setup

Plano-plano AT-cut quartz plates (14 mm in diameter) with a fundamental resonance frequency of 5 MHz (KVG, Germany) were coated with gold electrodes on both sides, each exhibiting an area of 0.265 cm<sup>2</sup>. The quartz resonator was placed in a Teflon chamber, exposing one side to a buffer solution and the other to air. The Teflon chamber was equipped with an inlet and outlet, and the aqueous circuit was driven by a peristaltic pump. An incorporated 1 ml reaction tube allowed the injection of proteins and substrates from outside of the Teflon chamber. The gold electrodes were connected to an electrical circuit, which was controlled by an oscillator circuit (SN74LS124N, Texas Instruments, USA). The entire system was thermostated in a Faraday cage at 34°C. The frequency change of the quartz resonator was recorded using a frequency counter (HP 53181 A, Hewlett Packard, USA) connected via RS 232 to a personal computer (Janshoff et al., 1996). Prior to use the gold surfaces the quartz plates were cleaned in an argon for 5 min (Plasma cleaner, Harrick, USA) before incubation in a 2 mM ethanolic solution of octanethiol for 30 min. Successful chemisorption was controlled by impedance spectroscopy (Steinem et al., 1997). The guartz resonators were rinsed thoroughly five times with ethanol and five times with buffer solution. Afterwards they were incubated with a 0.5 mg ml<sup>-1</sup> solution of LUVs at 50°C for 1 h. The lipid membrane was built by a selfassembly process, which was again controlled by impedance spectroscopy. Remaining lipids were removed by washing the guartz resonators 10 times with buffer solution. Finally, the Teflon chamber was placed in a Faraday cage, connected to the electrical circuit, and the aqueous circuit was closed by a nozzle.

# Surface functionalization and scanning force microscopy (SFM) imaging

Scanning force microscopy was performed using a multimode/Nanoscope IIIa (Digital Instruments, USA). The lipid membranes were transferred by a Langmuir-Blodgett transfer to mica sheets. In a first step, these mica sheets were hydrophobized by a DPPC monolayer at a surface pressure of 45 mN m<sup>-1</sup>. A DPPC/DPPG/CL/DPPS (75:18:5:2) monolayer was finally transferred, and the mica sheets were placed in buffer solution. Lipid layers were imaged in contact and tapping mode at 34°C. Commercially available silicone nitride tips (Park Instruments, USA) with pyramidal shape were used. The spring constants of the cantilevers were determined by the thermal noise method (Hutter and Bechhoefer. 1993). Typical spring constants were  $0.01 \pm 0.003~N~m^{-1}$ . Imaging was performed at a scan rate of 1 Hz with a typical load force of 100 pN.

#### WS/DGAT activity assays

Wax ester synthase/acyl-CoA:diacylglycerol acyltransferase activity was measured in QCM and SFM experiments in a total volume of 2.0 ml containing 30 µg ml<sup>-1</sup> purified WS/ DGAT (T. Stöveken, R. Kalscheuer and A. Steinbüchel submitted), 3.75 mM 1-hexadecanol or 3.75 mM 1,2-dipalmitoylglycerol, 4.63 mg ml<sup>-1</sup> BSA, 3.75 mM palmitoyl-CoA in 125 mM sodium phosphate buffer (pH 7.5). Hexadecanol/ BSA and 1,2-dipalmitoylglycerol/BSA were emulsified by ultrasonification. All QCM experiments were performed at 34°C and with a constant flow of 0.35 ml min-1 within the aqueous circuit. SFM experiments were also performed at 34°C.

#### **Acknowledgements**

The authors are grateful for financial support of the Deutsche Forschungsgemeinschaft (STE 386/7-2). We thank C. Büding, S. Wulff and M. Seidl for technical help and T. Lütke-Eversloh for critical discussions.

#### Supplementary material

The following material is available from http://www.blackwellpublishing.com/products/journals/ suppmat/mmi/mmi4441/mmi4441sm.htm

Fig. S1. Confocal Z-step scan images of cells of A. calcoaceticus ADP1 just beginning wax ester accumulation. Fig. S2. Confocal Z-step scan images of cell of A. calcoaceticus ADP 1 cultivated for 24 h under storage conditions.

Fig. S3. Confocal Z-step scan images of R. opacus PD630 cells in a starting phase of TAG accumulation.

Fig. S4. Confocal Z-step images of cell of R. opacus PD630 cultivated for 24 h under storage conditions.

Fig. S5. 3D-reconstitution fluorescent images A. calcoaceticus ADP1 cells from a cultivation stage just starting wax ester accumulation.

Fig. S6. 3D-images of cell of A. calcoaceticus ADP 1 cultivated for 24 h under storage conditions.

Fig. S7. 3D-images of R. opacus PD630 cells accumulating numerous lipid-prebodies. Lipid-prebodies occur as intensively stained peripheral lipid domains in direct association with the cytoplasm membrane.

Fig. S8. 3D-images of cell of R. opacus PD630 cultivated for 24 h under storage conditions exposing numerous faintly stained matured lipid-bodies inside their cytoplasm.

- Alvarez, H.M., and Steinbüchel, A. (2002) Triacylglycerols in prokaryotic microorganisms. Appl Microbiol Biotechnol 60: 367–376.
- Alvarez, H.M., Mayer, F., Fabritius, D., and Steinbüchel, A. (1996) Formation of intracytoplasmic lipid inclusions by *Rhodococcus opacus* PD630. *Arch Microbiol* **165**: 377– 386
- Alvarez, H.M., Kalscheuer, R., and Steinbüchel, A. (2000) Accumulation and mobilization of storage lipids by *Rhodo-coccus opacus* PD630 and *Rhodococcus ruber* NCIMB 40126. Appl Microbiol Biotechnol 54: 218–223.
- Arnold, M. (ed.) (1968) Histochemie. In *Einführung in die Grundlagen und Prinzipien der Methoden*. Berlin: Springer.
- Christensen, H., Garton, N.J., Horobin, R.W., Minnikin, D.E., and Barer, M.R. (1999) Lipid domains of mycobacteria studied with fluorescent molecular probes. *Mol Microbiol* 31: 1561–1572.
- Clausen, M.K., Kristiansen, K., Jensen, P.K., and Behnke, O. (1974) Isolation of lipid particles of Bakers-yeast. FEBS Lett 43: 176–179.
- Coleman, J. (1990) Characterization of Escherichia coli cells deficient in 1-acyl-sn-glycerol 3-phosphate acyltransferase activity. J Biol Chem 265: 17215–17221.
- Daniel, J., Deb, C., Dubey, V.S., Sirakova, T.D., Abomoelak, B., Morbidoni, H.R., and Kolattukudy, P. (2004) Induction of a novel class of diacylglycerol acyltransferases and triacylglycerol accumulation in *Mycobacterium tuberculosis* as it goes into a dormancy-like state in culture. *J Bacteriol* 186: 5017–5030.
- Dantuma, N.P., Pijnenburg, M.A.P., Diederen, J.H.B., and Van der Horst, D.J. (1998) Electron microscopic visualisation of receptor-mediated endocytosis of Dil-labeled lipoproteins by diaminobenzidine photoconversion. *J Histochem Cytochem* **46**: 1085–1089.
- Fixter, L.M., Nagi, M., McCormack, J.G., and Fewson, C.A. (1986) Structure, distribution and function of wax esters in Acinetobacter calcoaceticus. J Gen Microbiol 132: 3247– 3157.
- Garton, N.J., Christensen, H., Minnikin, D.E., Adegbola, R.A., and Barer, M.R. (2002) Intracellular lipophilic inclusions of mycobacteria in vitro and in sputum. Microbiology 148: 2951–2958.
- Huang, A.H.C. (1992) Oil bodies and oleosins in seeds. *Annu Rev Plant Phys* **43:** 177–200.
- Hutter, J.L., and Bechhoefer, J. (1993) Calibration of atomicforce microscope tips. Rev Sci Instrum 64: 1868–1873.
- Janshoff, A., Steinem, C., Sieber, M., and Galla, H.J. (1996) Specific binding of peanut agglutinin to Gm1-doped solid supported lipid bilayers investigating by shear wave resonator measurements. Eur Biophys J 25: 105–113.
- Janshoff, A., Galla, H.J., and Steinem, C. (2000) Mikrogravimetrische Sensoren in der Bioanalytik – eine Alternative zu optischen Biosensoren. Angew Chem 112: 4164– 4195.
- Jurasek, L., and Marchessault, R.H. (2004) Polyhydroxyalkanoate (PHA) granule formation in *Ralstonia eutropha* cells: a computer simulation. *Appl Microbiol Biot* **64:** 611– 617
- Kalscheuer, R., and Steinbüchel, A. (2003) A novel bifunc-

- tional wax ester synthase/acyl-CoA: diacylglycerol acyl-transferase mediates wax ester and triacylglycerol biosynthesis in *Acinetobacter calcoaceticus* ADP1. *J Biol Chem* **278:** 8075–8082.
- Kalscheuer, R., Wältermann, M., Alvarez, H.M., and Steinbüchel, A. (2001) Preparative isolation of lipid inclusions from *Rhodococcus opacus* and *Rhodococcus ruber* and identification of granule-associated proteins. *Arch Microbiol* 177: 20–28.
- Kalscheuer, R., Luftmann, H., and Steinbüchel, A. (2004) Synthesis of novel lipids in Saccharomyces cerevisiae by heterologous expression of an unspecific bacterial acyltransferase. Appl Environ Microbiol, doi:10.1128/ AEM.70.12.000-000.2004
- Lackner, K.J., von Landenberg, C., Barlage, S., and Schmitz, G. (2000) Analysis of prothrombotic effects of two human monoclonal IgG antiphospholipid antibodies of apparently similar specificity. *Thromb Haemost* 83: 583–588.
- Leber, R., Zinser, E., Zellnig, G., Paltauf, F., and Daum, G. (1994) Characterization of lipid particles of the yeast Saccharomyces cerevisiae. Yeast 10: 1421–1428.
- Leber, R., Landl, K., Zinser, E., Ahorn, H., Spök, A., Kohlwein, S.D., et al. (1998) Dual localization of squalene epoxidase, Erg1p, in yeast reflects a relationship between the endoplasmic reticulum and lipid particles. Mol Biol Cell 9: 375–386.
- Londos, C., Brasaemle, D.L., Schultz, C.J., Segrest, J.P., and Kimmel, A.R. (1999) Perilipins, ADRP, and other proteins that associate with intracellular neutral lipid droplets in animal cells. Semin Cell Dev Biol 10: 51–58.
- Mlíčková, K., Roux, E., Athenstaedt, K., d'Andrea, S., Daum, G., Chardot, T., and Nicaud, J.M. (2004) Lipid Accumulation, lipid body formation, and acyl Coenzyme A oxidases of the yeast *Yarrowia lipolytica*. Appl Environ Microbiol 70: 3918–3924.
- Muratsugu, M., Ohta, F., Miya, Y., Hosokawa, T., Kurosawa, S., Kamo, N., and Ikeda, H. (1993) Quartz-crystal microbalance for the detection of microgram quantities of human serum-albumin-relationship between the frequency change and the mass of protein adsorbed. *Anal Chem* **65**: 2933.
- Murphy, D.J. (2001) The biogenesis and functions of lipid bodies in animals, plants and microorganisms. *Prog Lipid Res* **40:** 325–438.
- Murphy, D.J., and Vance, J. (1999) Mechanisms of lipid-body formation. Trends Biochem Sci 24: 109–115.
- Napier, J.A., Beaudoin, F., Tatham, A.S., Alexander, L.G., and Shrewy, P.R. (2001) The seed oleosins: structure, properties and biological role. *Adv Bot Res* **35**: 111–138
- Olukoshi, E.R., and Packter, N.M. (1994) Importance of stored triacylglycerols in *Streptomyces* possible carbon source for antibiotics. *Microbiology* **140**: 931–943.
- Packter, N.M., and Olukoshi, E.R. (1995) Ultrastructural studies of neutral lipid localisation in *Streptomyces. Arch Microbiol* **164:** 420–427.
- Pötter, M., Müller, H., Reinecke, F., Wieczorek, R., Fricke, F., Bowien, B., et al. (2004) The complex structure of polyhydroxybutyrate (PHB) granules: four orthologous and paralogous phasins occur in *Ralstonia eutropha*. *Microbiology* 150: 2301–2311.

- Ratledge, C. (1989) Biotechnology of oils and fats. In Microbial Lipids. Ratledge, C., and Wilkinson, S.G. (eds). London: Academic Press, pp. 567-650.
- Reiser, S., and Sommerville, C. (1997) Isolation of mutants of Acinetobacter calcoaceticus deficient in wax ester synthesis and complementation of one mutation with a gene encoding a fatty acyl coenzyme A reductase. J Bacteriol **179**: 2969-2975.
- Robenek, M.J., Severs, N.J., Schlattmann, K., Plenz, G., Zimmer, K.P., Troyer, D., and Robenek, H. (2004) Lipids partition caveolin-1 from ER membranes into lipid droplets: updating the model of lipid droplet biogenesis. FASEB J **18:** 866-868.
- Sambrook, J., Fritsch, E.F., and Maniatis, T. (eds) (1989) Molecular Cloning. A Laboratory Manual, 2nd edn. Cold Spring Harbour, NY: Cold Spring Harbour
- Sauerbrey, G. (1959) Verwendung von Schwingquarzen zur Wägung dünner Schichten und zur Mikrowägung. Z Phys 155: 206-222.
- Schlegel, H.G., Kaltwasser, H., and Gottschalk, G. (1961) Ein Submersverfahren zur Kultur wasserstoffoxidierender Bakterien: Wachstumsphysiologische Untersuchungen. Arch Mikrobiol 38: 209-222.
- Sorger, D., and Daum, G. (2003) Triacylglycerol biosynthesis in yeast. Appl Microbiol Biotechnol 61: 289-299.

- Spurr, A.R. (1969) A low-viscosity epoxy resin embedding medium for electron microscopy. J Ultrastruct Res 26: 31-
- Steinbüchel, A. (1991) Polyhydroxyalkanoic acids. In Biomaterials, Novel Materials. Byrom, D. (ed.). Basingstoke: MacMillan, pp. 123-213.
- Steinem, C., Janshoff, A., Galla, H.J., and Sieber, M. (1997) Impedance analysis of the ion transport through gramicidin channels incorporated in solid supported lipid bilayers. Bioelectrochem Bioenerg 42: 213-220.
- Stubbe, J., and Tian, J. (2003) Polyhydroxyalkanoate (PHA) homeostasis: the role of the PHA synthase. Nat Prod Rep 20: 445-457.
- Tzen, J.T.Z., and Huang, A.H.C. (1992) Surface-structure of plant seed oil bodies. J Cell Biol 117: 327-335.
- Wältermann, M., Luftmann, H., Baumeister, D., Kalscheuer, R., and Steinbüchel, A. (2000) Rhodococcus opacus PD630 as a source of high-value single cell oil? Isolation and characterization of triacylglycerols and other storage lipids. Microbiology 146: 1143-1149.
- Wilkinson, W.O., and Bell, R.M. (1997) sn-Glycerol-3-phosphate acyltransferase from Escherichia coli. Biochem Biophys Acta 1348: 3-9.
- Zweytick, D., Athenstaedt, K., and Daum, G. (2000) Intracellular lipid particles of eukaryotic cells. Biochem Biophys Acta 1469: 101-120.